

pH-Sensitive Chitosan Hydrogel with Instant Gelation for Myocardial Regeneration

Alimirzaei F¹, Vasheghani-Farahani E^{1*}, Ghiaseddin A¹, Soleimani M², Pouri¹ and Zeinab Najafi-Gharavi³

¹Biomedical Engineering Division, Faculty of Chemical Engineering, Tarbiat Modares University, Tehran, Iran

²Hematology Group, Faculty of Medical Sciences, Tarbiat Modares University, Tehran, Iran

³Anatomical Sciences Group, Faculty of Medical Sciences, Tarbiat Modares University, Tehran, Iran

Abstract

Recently *in situ* injectable hydrogels have received considerable attention to regenerate failure heart tissue after myocardial infarction (MI). But two criteria remain crucial: first, defining their chemical composition and structural parameters because they must be fabricated to withstand physiological condition while having high cell retention; second, providing the hydrogel with short gelation time to protect the cells from washout and extrusion in the injection site. In this study, two different pH-sensitive hydrogels with instant gelation in the presence of aqueous acetic acid (WH sample), and DMEM medium along with acetic acid (MH sample) were prepared. The morphology and structural and mechanical properties of the hydrogels were evaluated by SEM, FTIR and compressive strength test, respectively. Also, the equilibrium swelling ratio of each hydrogel and their degradation rate as a desirable property were also determined. MTT test confirmed that both hydrogels were biocompatible and non-toxic for human Bone Marrow Mesenchymal Stem Cells (hBMSCs) within 14 days as well as 31 and 36% cell growth during this time for WH and MH samples, respectively. The viability investigation of human Adipose Mesenchymal Stem Cells (hADSCs), tested by live/dead assay with Acridine Orange and Ethidium bromide staining, showed high cell survival and cell density increase during 1, 7, 14, 21 days. The overall results demonstrated that both *in situ* forming hydrogels are promising candidates for regeneration of the infarcted myocardium.

Keywords: Injectable hydrogel; pH-sensitive; Chitosan; Instant gelation; Myocardial infarction

Abbreviations: MI: Myocardial Infarction; DMEM: Dulbecco's Modified Eagle's Medium; hBMSCs: Human Bone Marrow Mesenchymal Stem Cells; hADSCs: Human Adipose Mesenchymal Stem Cells; SEM: Scanning Electron Microscopy; FTIR: Fourier Transform Infrared Spectroscopy

Introduction

After myocardial infarction (MI), differentiated cardiomyocytes do not have the adequate ability of self-regeneration [1,2] that leads to necrosis and impaired cardiac function [2,3]. The ideal remedial method is heart transplantation that faces the crisis of donor shortage and recipients' rejections [4,5]. Hence, new cell-based therapy methods have emerged such as cell injection along with buffered saline or culture media into myocardium to regenerate the heart tissue [6]. But, this method often suffers from poor cell survival and lack of integration with native myocardium [2,7]. After injection, roughly 90% of donor cells would be lost due to washout and extrusion; moreover, remaining cells have only ~10% survival chance after 1 week [8]. Tissue engineering is novel and vital steps to enhance the efficiency of strategies for MI treatment [9] by providing temporary ECM to support cell growth during myocardial regeneration [10]. In this way, cell-laden hydrogels could provide an ideal microenvironment for proliferation and retention of cells injected to the infarcted area [7]. These systems are formed by physical or chemical cross-linking of water-soluble precursors, consisted of synthetic or natural polymers [11]. The conditions of gel formation, biocompatibility, biodegradability, injectability and providing adequate mechanical support are critical criteria for hydrogels design [12,13]. Furthermore, if gel formation is postponed, the biomaterial would not have any advantage over liquid-phase cell delivery [14]. Nowadays, numerous *in situ* forming hydrogels were utilized for myocardial regeneration in both *in vitro* and *in vivo* studies. These hydrogels are usually prepared from synthetic polymers like poly (trimethylene carbonate) [15], poly (ethylene glycol) [16], Poly

(N-isopropylacrylamide) [7,17] and natural polymers such as Alginate [18-20], gelatin [9,21], Fibrin [22], Hyaluronic acid [23], and in particular chitosan [24-28]. These investigations showed some advantages such as increasing left ventricular myocardial wall thickness, decreasing infarct size, preserving LV contractility, promotion of epicardial cell migration and angiogenesis. However, the major concern about synthetic hydrogels is potential cytotoxicity and their lack of biological cues such as cellular adhesion and interaction [1]. Also, natural hydrogels often suffer from low tunability, weak mechanical properties [7,29] leading to usage of toxic cross-linker to enhance mechanical robustness [30]. Additionally, they have roughly high gelation time even up to 1 h resulting in low cell retention and cell engraftment. To overcome the aforementioned obstacles and fulfill the necessary requirements, the aim of present study was to develop a pH-sensitive injectable hydrogel based on chitosan as a cell carrier, in accordance with cell niche, for myocardial regeneration.

It has been demonstrated that hydrogels based on chitosan, a cationic copolymer of (1→4)-2-acetamido-2-deoxy-β-D-glucan (N-AC-Glu) and (1→4)-2-amino-2-deoxy-b-D-glucan (D-glucan) units linked by (β(1→4) glycosidic bands, could improve MI microenvironment, especially enhance the retention and engraftment of Adipose Mesenchymal Stem Cells (ADSCs), due to its unique bioactive and antioxidant traits [2,31].

*Corresponding author: Vasheghani-Farahani E, Biomedical Engineering Group, Faculty of Chemical Engineering, Tarbiat Modares University, P.O. Box. 14115-114, Tehran, Iran, Tel: +98 21 82883338; Fax: +98 21 82885040; E-mail: evf@modares.ac.ir

Received October 21, 2017; Accepted October 28, 2017; Published November 10, 2017

Citation: Alimirzaei F, Vasheghani-Farahani E, Ghiaseddin A, Soleimani M, Pouri, et al. (2017) pH-Sensitive Chitosan Hydrogel with Instant Gelation for Myocardial Regeneration. J Tissue Sci Eng 8: 212. doi: [10.4172/2157-7552.1000212](https://doi.org/10.4172/2157-7552.1000212)

Copyright: © 2017 Alimirzaei F, et al. This is an open-access article distributed under the terms of the Creative Commons Attribution License, which permits unrestricted use, distribution, and reproduction in any medium, provided the original author and source are credited.

Therefore, the main objective of the present study was design of chitosan based hydrogels with instant gelation property for loading of ADSCs. For this purpose, design of experiments was applied for selection of proper condition for hydrogel preparation and extensive mechanical and physiochemical characterizations of the hydrogels, as well as *in vitro* investigation of cell survival in hydrogels were carried out.

Materials and Methods

Materials

Chitosan with molecular weight of 100-300 kDa and deacetylation degree more than 90% was purchased from Acros Organic (USA). Acetic acid, citric acid and disodium hydrogen phosphate were obtained from Merck (Germany). PBS, FBS, DMSO, DMEM medium, MTT kit and Trypsin were purchased from Gibco (USA). Acridine Orange, Ethidium Bromide dyes were purchased from Sigma- Aldrich, Steinheim (Germany).

Design of experiment

The response surface methodology (RSM) was used to optimize hydrogel formation with instant gelation, adjusting and stabilizing the pH of hydrogel at pH 7.4 (optimal physiological pH), having a minimal excess liquid left after gel formation to yield a gel with desirable mechanical properties and cell survival. Central composite design (CCD) with 30 runs (6 center points, 16 factorial points and 8 axial points) was applied at 5 levels. Four independent variables including normality and volume of NaOH to be used for gel formation and volume and pH of buffer solution were selected as most important variables. All factors levels were determined based on preliminary experiments. The dependent variables as the responses of experimental design were pH of hydrogel and excess liquid left after gel formation. The Design-Expert7.0 software was used for regression and graphical analysis of the obtained data. Table 1 shows different factors with corresponding levels. The details of designed experiments are presented in Table S1 of supplementary materials.

Preparation of chitosan hydrogels

Two chitosan solutions 1% (w/v) were prepared by dissolving

chitosan powder in aqueous acetic acid 1% (w/v), (WH sample), as well as DMEM medium along with acetic acid 1% (w/v), (MH sample), at room temperature and stirring for 5 h. The initial pH of solutions was acidic (pH 4-5) and adjusted around 6.8-6.9 by drop wise addition of NaOH (10 N) to the stirring solution. For gel formation, NaOH solution (0.75N) was added to the stationary solution. However, before NaOH addition, a buffer solution (pH 6) of Na₂HPO₄ and citric acid was added to prevent abrupt pH changes of hydrogel precursor solutions.

Fabrication of injecting needle

As shown in Figure 1A, to inject hydrogel precursor and NaOH solutions into myocardium, a coaxial needle was designed for *in situ* hydrogel formation through simultaneous mixing of the solutions. Also, a 1 ml insulin syringe and a 20 ml syringe (Figure 1B) were used to pump NaOH and hydrogel precursor solutions through corresponding needles, respectively.

Scanning electron microscopy (SEM)

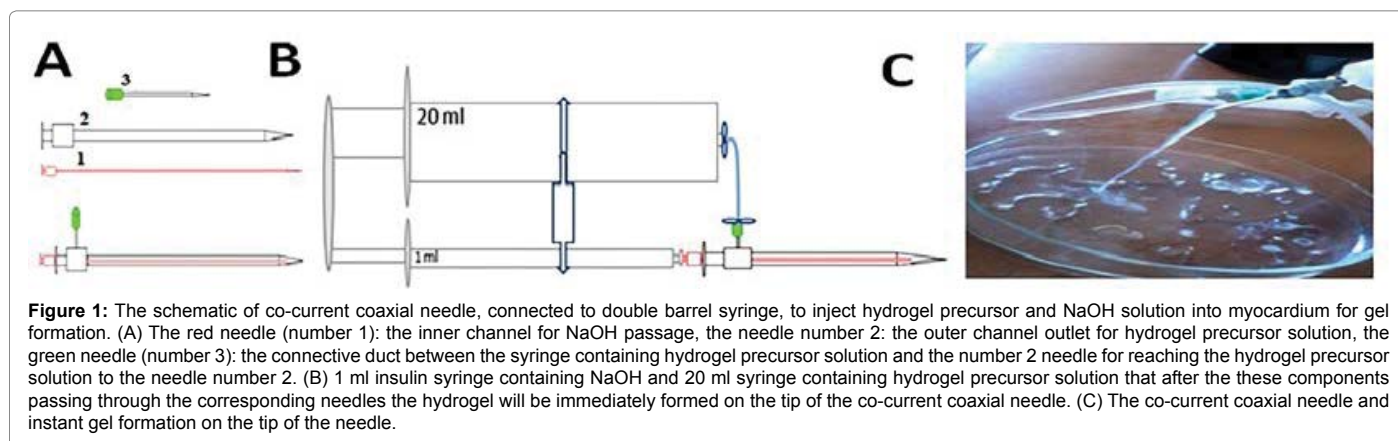
To study the morphology and the pore structure of the hydrogels, the samples were immersed in PBS at 37°C, removed after 1 and 10 days and frozen at -80°C followed by lyophilization (Zibrus technology GmbH, Germany) within 72 h; then, coated with gold and scanned at an accelerating voltage of 20 kV. The morphology of freeze-dried samples studied by taking SEM (Seron, AIS-2100, Korea) images. The average pore diameter of the hydrogels was acquired by measuring about 100 pores for each sample with image J software (version 1.44p national institute of health).

Fourier transform infrared spectroscopy (FT-IR)

FT-IR spectroscopy analysis was performed to identify the structural difference between the initial chitosan powder and ultimate products, MH and WH samples. Briefly, all samples were dried in vacuum oven during 72 h (BINDER GmbH, Germany), then shattered and mixed with potassium bromide in 1:100 ratios. The mixture was compacted to 1 mm semitransparent disk by exerting 20 MPa pressure for 5 min. The FT-IR spectra in wavelength range of 4000-400 cm⁻¹ were acquired applying a FT-IR spectrometer (Thermo Nicolet, NEXUS-760, USA) [32].

(α-) level	(1-) level	0)central level	(+1)level	(α+)level	Factor	code
0.5	0.63	0.75	0.88	1	Normality of NaOH (mol/l)	A
4	8	12	16	20	Volume of NaOH (μl)	B
6	6.2	6.4	6.6	6.8	pH of buffer	C
5	10	15	20	25	volume of buffer (μl)	D

Table 1: Variables and levels selected to prepare *in situ* forming hydrogels from 200 μl chitosan precursor solution (1% w/v).



Compressive strength of hydrogel

Because the tensile test is not suitable for the hydrogels, compressions tests were performed on cylindrically-shaped samples to determine the elastic modulus [33]. Hydrogels samples were prepared as described before and compressed between two compression plates under 0.02 MPa pressure with a rate of 5 mm/min at room temperature (n=3) using a compression instrument (Santam, STM-20, Iran). Stress-strain curve was drawn and Young's modulus was calculated to show mechanical strength of the samples [15].

Viscosity of hydrogel precursor solutions

For investigation of injectability, the viscosity of chitosan precursor solutions was measured at 30°C (n=3) using viscometer (Brookfield, DV-III Ultra, USA) [34].

Hydrogel degradation

To evaluate the degradation of hydrogels, 5 holes were punched on the caps of 2 ml Eppendorf tubes with a 17G needle and hydrogel samples were prepared from 500 µl precursor solutions in each tube [8]. Then 1 ml of DMEM medium was added to each tube, incubated in shaker incubator at 100 rpm and sampled at 1, 24, 48, 72, 120, 240 h (n=3 per time point) with medium changes (1 ml removed and replaced with fresh medium) every 48 h. For sampling, 1 ml of medium was removed from the tubes and gels were frozen at -80°C. Finally, all samples were lyophilized together for 72 h and weighed again. Weight loss percentage defined by comparison of the lyophilized gel weight to that of the 1 h groups [8].

Swelling studies

Hydrogel samples were prepared and lyophilized. The swelling behavior of samples was determined by immersing them in phosphate buffer saline (pH 7) at 37°C. Over a period of 24 h the samples were weighted at specific time intervals (n=3 per time point) until a constant weight was reached. Then, the swollen samples were blotted with filter papers to absorb excess water on their surface and weighted immediately [32]. The swelling ratios, Q, were calculated as quotient of the swollen gel weight and the dry polymer weight [35].

MTT cytotoxicity assay

The hydrogel samples from 100 µl of two different precursor solutions were prepared in each well of 96 wells plate and almost 100,000 hBMSCs, provided by Tehran Heart Center (Iran), were seeded on the surface of each hydrogel sample. The samples were incubated in DMEM, supplemented with 10% FBS, under standard cell culture conditions. Then hydrogel cytotoxicity was investigated by MTT-assay (Gibco, USA) after 0 (the first culture day), 1, 3, 7, 14 days of incubation (n=5 per time point). The culture medium was changed every 3 days [36].

Cell loading

The hADSCs (provided by cell bank of Bon-Yakhte Research Center in Tehran, Iran) were suspended in 70 ml of both chitosan solutions (1 million/ml) and hydrogel samples were prepared by mixing of cell loaded chitosan solutions and NaOH (0.75 N). These cell loaded hydrogels were transferred to 96 well plates and cultured for 21 days. Each well contained 100 µl of culture medium and refreshed every 2 days.

Live/dead assay

Cell viability and apoptotic potential were investigated through live/dead assay using Acridin orange ethidium bromide (AO/EtBr)

staining (Sigma-Aldrich, Steinheim, Germany), and cells were imaged with a fluorescent microscope (Nikon, TE 2000-S, Japan). It should be noted that the nucleuses of live cell and dead cells become green and red with AO and EtBr, respectively [36].

Statistical analysis

The data were analyzed using one-way ANOVA with post hoc Tukey tests or two-way t-test statistical method. All data being reported as mean ± standard deviation (SD). At least three groups were compared in each Statistical analysis. A value of p<0.05 was considered statistically significant.

Results

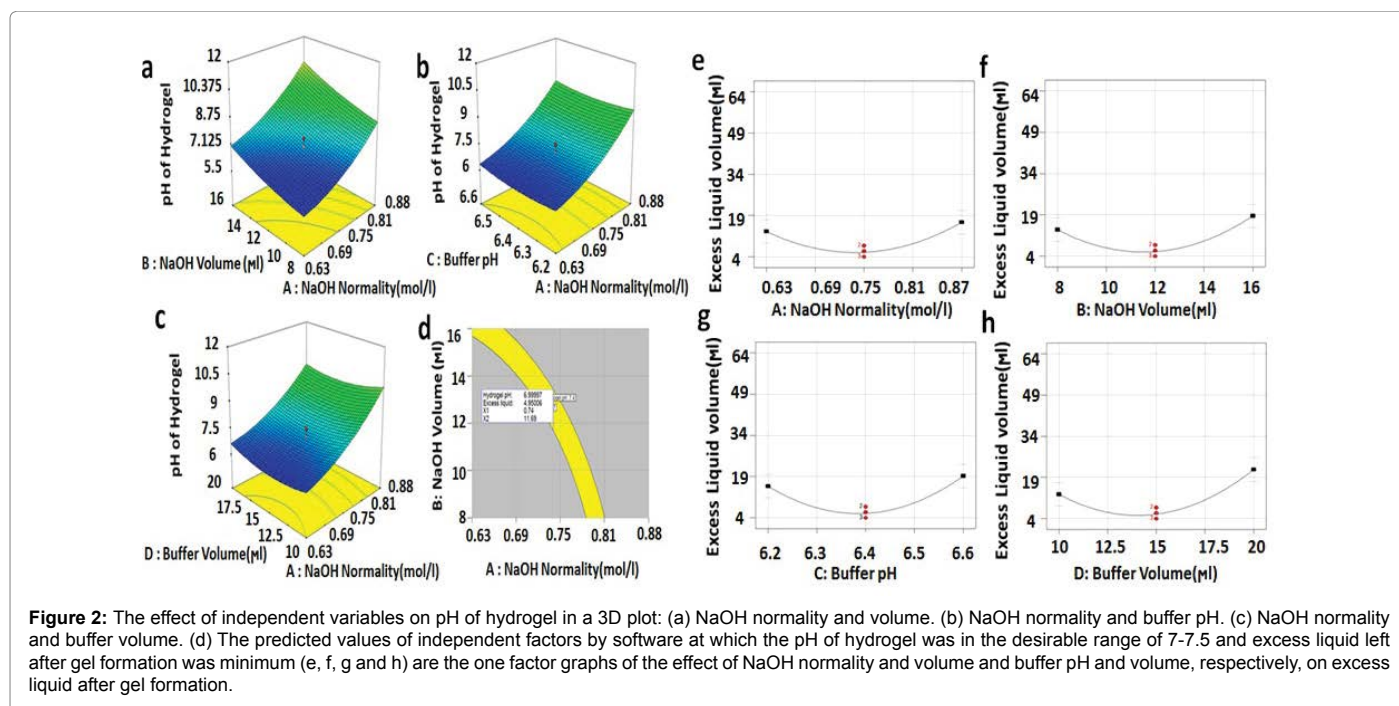
Design experiments

The conditions of different experimental runs for independent factors and corresponding responses are presented in Table S1 of the supplementary material. The gelation process was optimized by empirical data correlation using design Expert-7.0 software. A quadratic model, Y_1 , for response 1 (pH of hydrogel) and a modified quadratic model, Y_2 , for response 2 (excessive liquid left after gel formation) were suggested to correlate dependent variables of Y_1 and Y_2 to independent factors. The final equations for pH of hydrogel [Eq. (1)] and for excess liquid [Eq. (2)] in terms of coded factors are presented, where A, B, C and D are coded values of NaOH normality, NaOH volume, pH of buffer and volume of buffer, respectively.

The analysis of variance (ANOVA) for hydrogel pH and excess liquid left after gelation, summarized in Tables S2 and S3 of supplementary material respectively, indicates that the results are statistically significant for both dependent variables with p-value<0.0001.

$$Y_1 = 7.17 + 1.56A + 0.85B + 0.021C - 0.021D + 0.094AB - 0.031AC - 0.16AD - 0.16BC - 0.031BD + 0.094CD + 0.52A^2 + 0.2B^2 + 0.2C^2 + 0.39D^2 \quad (1)$$
$$Y_2 = 5.67 + 1.67A + 2.5B + 1.83C + 4.5D - 2.75AD + 2.25BD + 9.21A^2 + 10.46B^2 + 11.71C^2 + 11.71D^2 \quad (2)$$

Figures 2A-2C show the effect of independent factors on pH of hydrogel in a three dimensional graph obtained from Design Experiment Software. According to Figure 2A, pH of hydrogel increased by increasing both the normality and volume of NaOH as expected. The effect of NaOH normality is more than that of NaOH volume changes because of the reduced volume of the final mixture at gel formation. The higher value for constant coefficient of NaOH normality (A) in Eq. (1) agrees well with this result. As shown in Figures 2B and 2C the effect of buffer pH and volume on hydrogel pH was not significant due to its buffering capacity. Figures 2E-2H shows the effect of four independent factors on the excess liquid left after gel formation. As shown in these figures, the amount of excess liquid decreased to a minimum value by increasing all factors and then increased by further increase of them. The decrease of excess liquid is due to higher gel formation in a mixture with appropriate pH for hydrogen bonding and electrostatic interaction between polymer chains. Figures 2E and 2G indicate that by further increase of NaOH normality and buffer pH, the pH of chitosan solution increased with consequent decrease of electrostatic interaction and hydrogen bonding between polymer chains which in turn reduced gel formation with increase excess liquid. Further increase of NaOH volume (Figure 2F) enhances pH and volume of final chitosan mixture with consequent decrease of electrostatic and hydrogen bonding between polymer chains and resulted in less gel formation with increase of excess liquid. Excessive dilution of chitosan solution by further increase of



buffer volume (Figure 2H) resulted in less electrostatic interactions and hydrogen bonding between polymer chains with consequent decrease of gel formation and increase of excess liquid.

Based on these results, the optimum condition at which the pH of hydrogel was in the desirable range of 7-7.5 with minimum excess liquid was determined. The yellow region in Figure 2D indicates the predicted area for the favorable responses by desirability of 0.923. As shown in this figure, the optimum values of NaOH normality and volume, buffer pH and volume were 0.74 mol/l, 11.69 μ l, 6.38 and 14.01 μ l, respectively. At optimum condition the pH of hydrogel and the volume of excessive liquid was 7 and 4.95 μ l, respectively. However, the corresponding experimental values of the conformation test were 7-7.5 and 7 μ l, respectively.

Adjustment of hydrogel pH and instant gel formation on the needle tip

The pH of hydrogels, prepared at optimum condition, was appropriately adjusted to be in the range of 7-7.5 as typical pH of 6.8 to 7.6 for cell culture [37] and pH of 7.0-7.4 for the highest specific growth rate [38]. Also, as shown in Figure 1c, a co-current coaxial needle was built in which the hydrogel precursor solution (plus cell in cellular investigations) flows through the external conduit and NaOH as a gellant passes through internal needle. The aforementioned solutions reach simultaneously to the needle tip and hydrogel forms instantly without any cell and material wasting.

SEM analysis

The SEM images for MH and WH were taken from samples that were removed from PBS after 1 and 10 days after immersion at 37°C and completely freeze dried. Figures 3A and 3D show that both samples were porous with almost homogenous porosity with the average pore size of 14.69 and 17.43 μ m for the WH and MH samples at day 1, respectively. However, Figures 3C and 3F show the formation of large gaps and enlargement of the pores up to 500 μ m because of gradual

hydrogel collapse and disintegration after 10 days' immersion in PBS for the WH and MH samples, respectively.

FT-IR analysis

The FT-IR spectra of initial chitosan powder, dried WH Hydrogel and dried MH hydrogels are shown in Figure 4A. Chitosan characteristic absorptions were located at 663 cm^{-1} related to C—H stretching vibration. The bands at 1034 and 1091 cm^{-1} belong to secondary hydroxyl group (typical peak of —CH—OH in cyclic alcohols, C—O stretch) and the primary hydroxyl group (characteristic peak of —CH₂—OH in primary alcohols, C—O stretch) [32]. The peaks at 1380 and 1423 cm^{-1} related to N—H stretching (amid III band) and N—H stretching of amide and ether bonds, respectively [32]. The bands at 1595 and 1658 cm^{-1} ascribed to bending variation of the N—H (N-acetylated residue, amide II band) and the carbonyl (C=O) stretching in amide I, respectively [32]. The absorption bands at 2877 cm^{-1} related to typical stretching of C—H [39]. and the peaks at 3179 cm^{-1} pertaining to O—H stretching and N—H stretching of chitosan [32]. FTIR spectra of WH hydrogel showed bands at 517, 643, 851 and 1093 cm^{-1} that are attributed to bending and symmetric stretching of PO₄³⁻ and P—O [40] in the used buffer. It should be noted that peaks at 643 and 1093 cm^{-1} were respectively connected to C—H and C—O stretching of chitosan as well, but it is difficult to differentiate them because of overlapping with the bands of phosphate groups. The absorption at 1412 and 1562 cm^{-1} are related to N—H stretching of amide III and amide II of chitosan. The bands at 1640 and 1697 cm^{-1} connected to C=O stretching of chitosan. The peaks at 2871 cm^{-1} related to stretching of C—H and finally the accumulated peaks at 3182, 3293 and 3421 cm^{-1} belong to N—H symmetrical vibrations concerned with Amide II that exists in N-acetyl glucosamine unit of chitosan and vibration of O—H of chitosan [39] and additive materials. FTIR spectra of MH hydrogel showed bands at 518, 643, 833 and 1022 cm^{-1} attributed to bending and symmetric stretching of PO₄³⁻ and P—O of the used buffer and also culture medium in this hydrogel. Similar to spectra of WH hydrogel, it should be considered that peaks at 643 and 1093 cm^{-1} were also related to C—H and C—O stretching

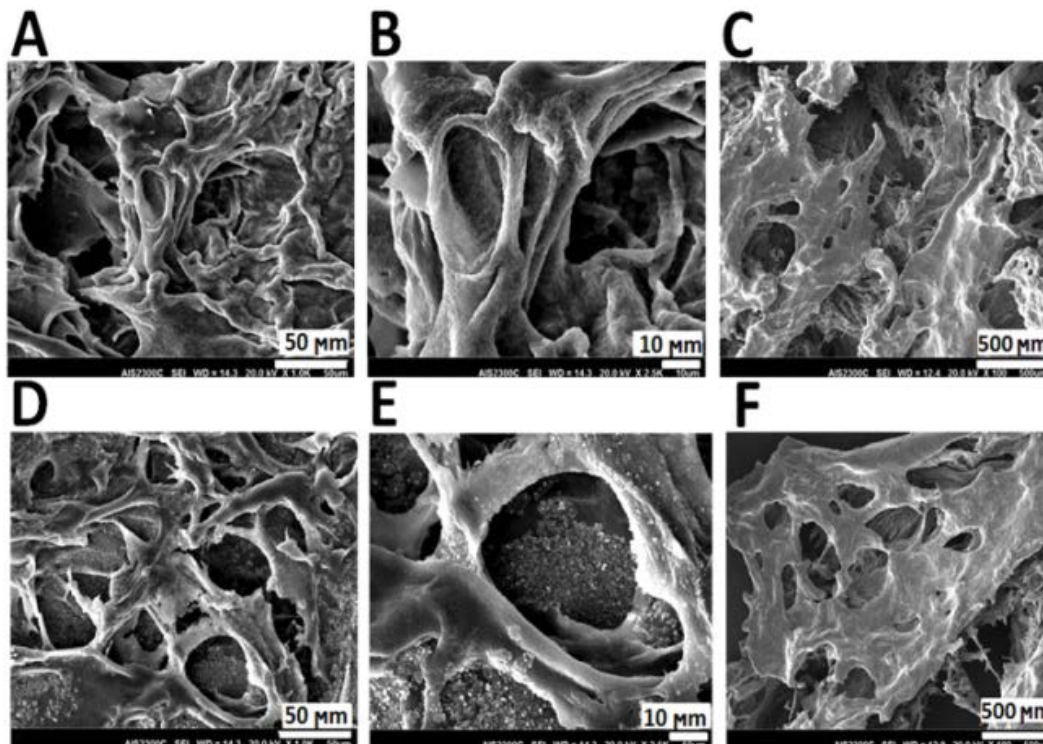


Figure 3: The SEM images of freeze dried hydrogels morphology and porosity with different magnification. (A) and (B) WH sample, (D) and (E) MH sample after 1 day immersion in PBS. (C) WH sample and (F) MH sample after 10 days' immersion in PBS.

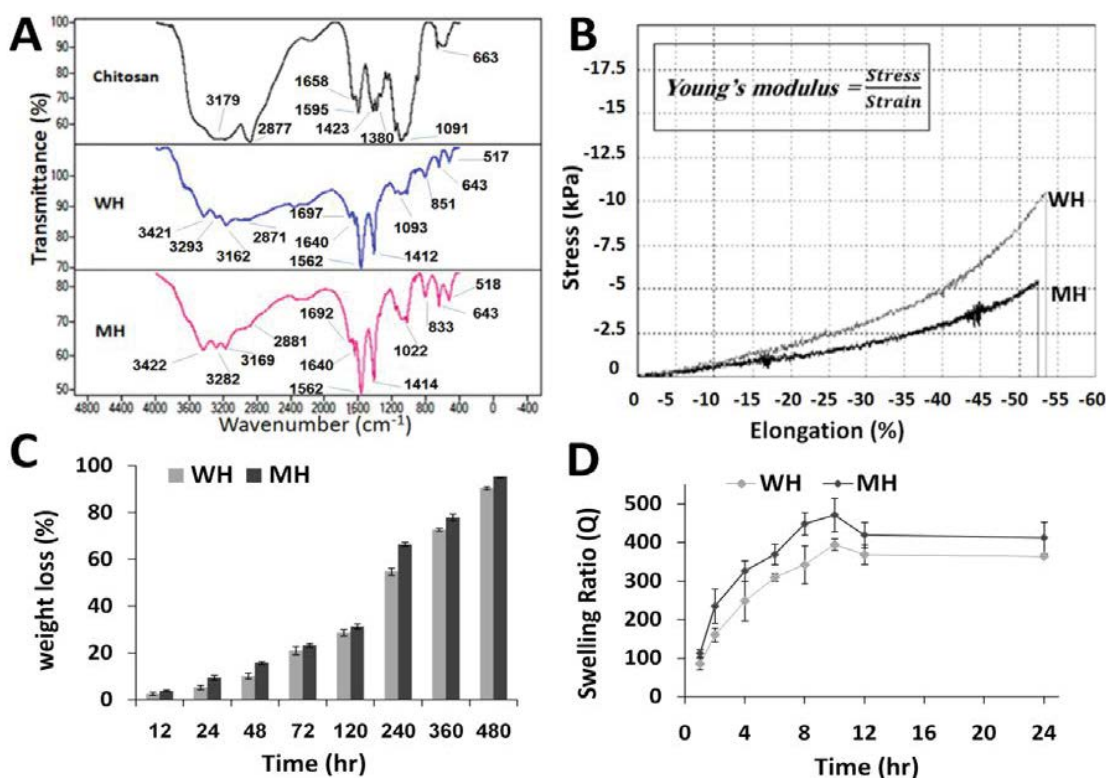


Figure 4: Physicochemical and mechanical characterization of hydrogels: (A) The FT-IR spectra of chitosan and prepared hydrogels. (B) The stress- strain curve from compression test for different samples. (C) The weight loss of hydrogel within 20 days of immersion in DMEM at 37°C. (D) The swelling ratio of hydrogels; WH: Sample prepared with water. MH: sample prepared with medium.

of chitosan, but it is difficult to differentiate them due to the overlaps with the bands of phosphate groups. The absorption at 1414 and 1562 cm^{-1} belong to N—H stretching of amide III and amide II of chitosan. The bands at 1640 and 1692 cm^{-1} are connected to C=O stretching of chitosan. The peaks at 2881 cm^{-1} attributed to typical stretching of C—H and eventually the collected peaks at 3169, 3282 and 3422 cm^{-1} belong to N—H symmetrical vibrations concerned with amide II that exists in N-acetyl glucosamine unit of chitosan and vibration of O—H in chitosan and additive materials [39]. In both hydrogel samples after NaOH addition, the intensity of C—O bands with the centrality $\sim 1090 \text{ cm}^{-1}$ and C—H bands with the centrality $\sim 2880 \text{ cm}^{-1}$ became low; because CH_3COONa salt is formed by NaOH addition and the intensity of C—O an C—H peaks decreased. In areas corresponding to the N—H stretching and the carbonyl group in the range of 1560 to 1690 cm^{-1} were intensified because of the presence of carbonyl groups of citric acid in the buffer, and the acetic acid in the aqueous solvent which is used to dissolve chitosan. Also, the presence of hydroxyl groups in the additive materials increased the accumulation of the —OH peaks in the range of 3000 to 3500 cm^{-1} . Furthermore, since the peaks around 893 to 1156 cm^{-1} are generally related to saccharide structure [39]; and the peaks around 517 to 1093 cm^{-1} in both hydrogels were connected to phosphate group. As shown in Figure 4A, the peaks of the MH sample in these ranges were intensified due to the presence of further carbohydrate and phosphate groups in DMEM used in this sample, compared with WH sample. It should be mentioned that the weakness of C—H peaks intensity with centrality $\sim 2880 \text{ cm}^{-1}$ is because of the high deacetylation degree of chitosan and this feature enhances the adhesion of cells due to the high amine groups on chitosan [41].

Mechanical strength and elastic modulus of hydrogels

The mechanical properties of hydrogels, determined by compressive strength test are shown in Figure 4B. The peak stress for WH and MH samples, which is equal to the average of maximum stress just before hydrogel break and disruption, was 10.6 and 5.5 kPa, respectively. The strain of hydrogels, determined by dividing the change in length to the initial length of hydrogel samples, was 53.4 and 52.6% for WH and MH samples, respectively that indicates the samples' flexibility. Finally, the elastic modulus (Young's modulus) of WH and MH samples, obtained by dividing stress to strain, was 19.8 and 10.3 kPa, respectively. By and large, the mechanical property of MH sample was weaker than that of WH sample that can be attributed to the presence of mineral salts in hydrogel precursor solution which reduces the interaction between polymeric chains. The more interactions between polymeric chains cause the more physical cross-linking with consequent increase of the mechanical strength [15]. Besides, the SEM images in Figure 3 show that the pore dimension and extent of hydrogel disintegration for MH sample were more than those of WH sample that acknowledge its less mechanical strength of MH sample.

Hydrogel degradation

Figure 4C shows the weight loss of WH and MH samples in DMEM versus time. Both hydrogels were susceptible for gradual weight lost in DMEM solution due to solvent penetration with increased swelling pressure against mechanical strength emerged by physical cross-linking points of the polymeric network. So the structural integrity of the physically and ionically cross-linked hydrogels decreased gradually, hydrogels crumbled and collapsed in the media. Also, gel-sol transition occurred simultaneously due to slight and gradual decrease of ambient pH to 6.5 with consequent weight loss of hydrogels. As shown in Figure 4C, the weight loss of both samples in the early hours was low due to

the integrity of the gel structure, but disruption and gel-sol transition increased gradually and after 20 days the weight loss of MH samples was more than 90%. Similar trends can be observed for WH sample. The mechanical strength test, samples morphology and porosity endorsed the more weight loss of MH sample.

Swelling ratio

Swelling ratio of hydrogels is shown in Figure 4D. According to these results, the rate of solvent absorption by both samples was initially high and decreased gradually until reached to the maximum swelling ratio after 10 h. Then, swelling ratios started to decrease due to the slight decrease of swelling pressure and the equilibrium swelling ratios were 360 and 415 for WH and MH samples after 12 h, respectively. The higher swelling ratio of MH sample, compared with that of WH sample, can be attributed to its weak mechanical strength.

Viscosity of chitosan solutions

The viscosity of hydrogel precursor solutions was 12.5 and 20 cp for WH and MH samples, respectively. The higher viscosity of MH sample is due to the presence of mineral salt in precursor solution. Collectively, these results indicate that the viscosity of both WH and MH samples was suitable for *in situ* gel formation since the viscosity of injectable hydrogels must be below 50 cp [30] to be injected easily into the body at liquid state.

Cytotoxicity of hydrogels

Figure 5 shows the cytotoxic effect of hydrogels on hBMSCs that were seeded on their surface via MTT-assay during 14 days. The survival of cells is reported in terms of optical density (OD) at 570 nm. These results show that the hydrogels were nontoxic and biocompatible for hBMSCs, as well as 31 and 36% cell growth during this time for WH and MH samples, respectively. The OD and proliferation of cells seeded on MH sample was more than that for WH sample, because it contained culture medium during gel formation. Based on time standard, it can be said that both hydrogels were nontoxic and biocompatible as 75% of the primary cells survived at the end of MTT test [42].

Cell viability

Figure 6A shows the AO/EtBr staining results for hADSCs loaded into hydrogel samples after 1, 7, 14 and 21 days of cell culture. As shown in these figures, most of the observed cells were alive, dispersed and stretched well in hydrogels. Live/dead staining showed excellent survival rates of cells. Viability percentages of hADSCs cultured in MH samples on day 1, 7, 14 and 21 were 90.76, 95.45, 94.97, 96.78% and in WH samples were 87.5, 95.04, 91.30 and 99.56%, respectively. Although

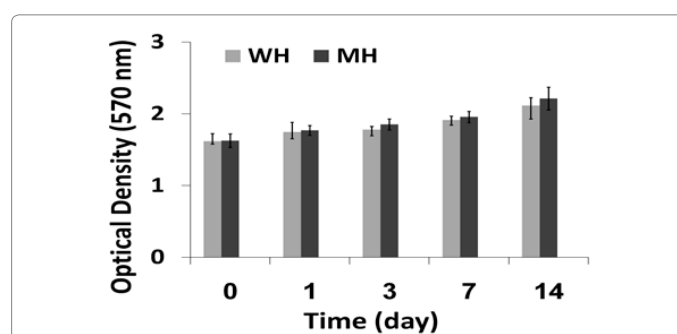


Figure 5: Cell survival in terms of optical density vs. time at 0 (first culture day), 1, 3, 7, 14 days of post-seeding, determined by MTT assay.

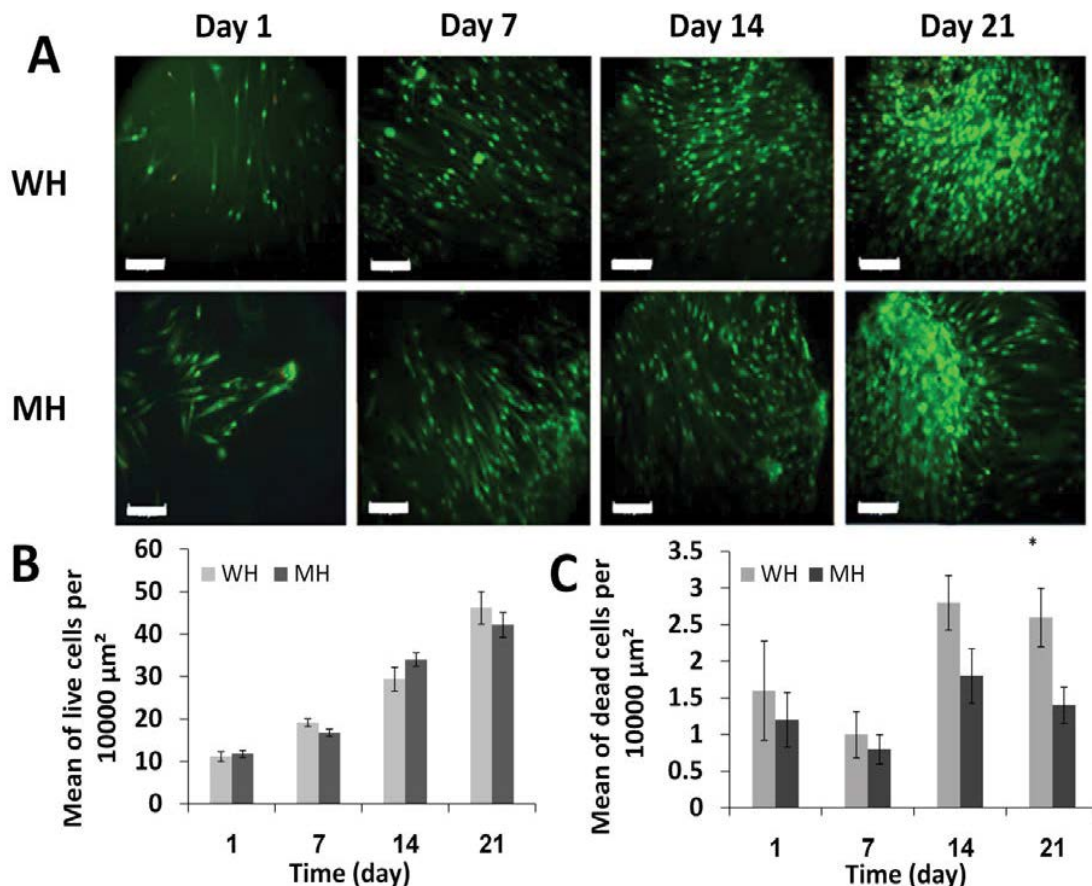


Figure 6: The viability of hADSCs, loaded into hydrogels. (A) AO/EtBr staining and fluorescent images (green (live) and red (dead)) of hADSCs loaded in two type chitosan hydrogels on different days of post-culturing (Scale bar represent 50 μm). (B) Proliferation of hADSCs cultured in chitosan hydrogels during 21 days. There was no significant difference between two types hydrogel (n= 5; Mean ± SE). (C) Dead hADSCs cultured in chitosan hydrogel during 21 days. *significant difference between two samples on the 21th day of culturing (P ≤ 0.05; n=5; Mean ± SE).

the difference between the number of viable cells of both samples was not significant (Figure 6B), the number of dead cells showed significant difference ($p \leq 0.05$) on the 21st day of culturing (Figure 6C).

Discussion

Despite contemporary hydrogels provide an acceptable matrix for delivering exogenous cells to the infarct zone, most of them suffer from low adjustability such as dearth of cell retention, roughly high gelation time and inadequate mechanical properties [7]. In particular, the vast number of former researches on injectable hydrogels has focused on animal studies without meticulous material characterizing and *in vitro* analyses to define an optimal fabrication according to physiological condition. Thus, this is vital to perform extensive analyses on fabrication multifaceted desirable hydrogel prior to *in vivo* experimentations.

In this work, two pH-sensitive hydrogels based on chitosan were prepared in the presence of aqueous acetic acid and DMEM medium (as helper nutrient for cells) along with acetic acid, to overcome the above mentioned constraints. Chitosan, a cationic naturally-derived biomaterial with high hydrophilicity, was chosen because of its structural similarity to glycosaminoglycans, a pivotal constituent of the ECM that enhanced cell viability for many types of cells [12]. Also, appropriate combination of chitosan with various cells, especially ADSCs, has been confirmed according to literatures [2,31]. However,

chitosan suffers from mechanical weakness and instability [12]. To have an instant gelation in aqueous solutions and enhance the mechanical robustness, NaOH was selected as a strong base, to provide physical crosslinking between chitosan polymeric chains by hydrogen bonding. Also, to prevent the drastic increase in the pH of hydrogel, unique phosphate buffer was utilized to adjust the pH of hydrogel around 7.4 as an optimal physiological pH. In addition, this phosphatic enhancer was applied with the aim of inducing ionic intermolecular interactions and consequently elevating mechanical properties and controlling degradation time of hydrogels.

As shown in Figure 4A, presence of all typical absorptions of chitosan and characteristic bands of phosphatic groups of the buffer in both hydrogels indicates all amino polysaccharide nature and properties of chitosan were maintained in comparison to pure chitosan before gel formation. So, fluctuations caused by the addition of buffer and NaOH leading to hydrogen bonds and intermolecular ionic interactions between positive charge of chitosan and negatively charged ions of the buffer and sodium hydroxide, but no covalent bonds were observed in gel formation process that indicate hydrogels were formed through physical and ionic gelation [41]. As seen in Figure 1C, after combination of these components on the tip of designed unique co-current coaxial needle, hydrogel formed immediately via these favorable intermolecular interactions. In most of the previous studies [43], because of the slow gel formation even up to 1 h, the injected cells and materials were more

seemingly to be completely washed out in the heart's severe contracting environment, and carried away in the bloodstream than to be a suitable gel in the ventricle wall [1]. So, such a rapid instant gel formation with least washout and cell wasting in the injection site is a promising achievement. Furthermore, the combination of the selected components and the molecular interactions between them without covalent cross-linking provided desirable degradation rates for the hydrogels. Actually, two mechanisms were responsible for degradation of the hydrogels: disruption and gel-sol transition. The hydrogels immersed in DMEM gradually collapsed as well as becoming soluble due to the decrease of medium pH to 6.5 at which sol-gel transition occurred. Hydrogels for cardiac repair should survive for at least one week and be totally removed in 6 weeks [44]. Thus, a degradation time of 20 days (Figure 4C) for the samples with fundamental goal of delivering into and preserving cells in injured region is suitable time; because, it is not too short causing leaking out of the cells and not so long resulting in spatial hindrance and preventing revascularization. As can be observed in SEM images of Figure 3, the trend of hydrogel degradation affected its architecture and porosity. At first day of immersion in PBS, the average pore size of MH and WH samples was 14.69 and 17.43 μm (Figures 3B and 3E), respectively. As the dimension of myocardium pores are about 20 μm [21], both samples seemed suitable for myocardial regeneration because required oxygen and nutrients for cells growth could easily pass through these hydrogels. Figures 3C and 3F show the formation of large gaps and enlargement of the pores up to 500 μm because of gradual hydrogels collapse and degradation after 10 days of immersion in PBS. This is a desirable structural property of hydrogel for cell growth and proliferation with simultaneous tissue regeneration; because the cells will have more spaces for growth and receive more nutrients and oxygen through these large pores to increase their population until complete regeneration [45].

Hydrogels are distinguished as ideal environments for cell and tissue growth due to their high water contents and soft tissue-like elasticity [46]. Particularly, swelling of hydrogel based on chitosan has direct relation with hydrophilicity of constituent groups [32]; and ionization of anionic and cationic groups of the network into chitosan's polymeric chains and higher swelling ratio is favorable for transfer of nutrients required for encapsulated cell growth [47]. Equilibrium swelling ratio of WH and MH hydrogels was 360 and 415, respectively and were considerably higher than those reported by Dahlmann et al. for hydrogels used for cardiac regeneration [35]. Additionally, such high water content along with the presence of good intermolecular interactions through physical and ionic gelation caused favorable mechanical robustness and elasticity for both samples in accordance with native cardiac tissue. The compressive elastic modulus (Young's modulus) of hydrogels for cardiac repair should be at least in the range of 10 to 15 kPa [21] for comparison, the modulus of heart tissue is 5.8 kPa [30]. Thus, the suitable compressive elastic modulus of hydrogels makes them a good candidate for myocardial regeneration and also it has been shown the Young's modulus of hydrogel and cardiac differentiation of stem cells have direct relation [15]. The elastic modulus of WH and MH samples was 19.8 and 10.3 kPa, respectively, which fulfill the required amount, and are flexible enough to resemble heart muscle. However, it can be said, in this case, WH sample with more elasticity may be a better candidate to be used for cardiomyocyte regeneration.

MTT results confirmed that applied materials not only did not have adverse effect on hBMSCs, but also were very biocompatible for cell retention and viability (Figure 5). Live/dead staining of hADSCs substantiated that the pH of hydrogel samples was adjusted very well in the pH range for cell viability. Both hydrogels maintained hADSCs

viability during 21 days of culturing that was almost greater than 88 and 91% for WH and MH samples, respectively. These results confirmed the FTIR analysis that chitosan structure maintained after gel formation; because it is well known that protonated amine groups of chitosan interact with negatively charged cell membranes and cause cell adhesion and growth [48]. In addition to pH one of the important factors of physiological environment is its osmolality. When a mammalian cell is exposed to a hypertonic surrounding the water will leave the cell leading the cell to shrink. Conversely, when this cell is subjected to a hypotonic surrounding, the water molecules will penetrate into the cell causing the cell to swell. As seen in Figure 6A, all cells in both samples had stable and normal shape during culture days. This clarifies the fact that the used buffer properly mimicked physiological buffer. In fact, the internal and external osmotic pressure of cells resembled the physiologic pressure and consequently the cells became neither shrinkage nor swollen. Collectively, these results indicated that cell viability for MH samples was more than that for WH samples due to more access of cells to nutrients in culture media that existed in MH hydrogels especially in the early hours of culture or during a long time. Also, higher porosity and more spaces for cell growth in MH samples provided free movements and migration of cells with consequent more growth and proliferations during cell culture.

Conclusion

In this study, two pH-sensitive chitosan hydrogels were prepared in the presence of aqueous acetic acid and DMEM culture medium, and tested as cell carrier and cardiac scaffold for regenerating of infarcted myocardium. The combination of chitosan, NaOH and applied phosphate buffer provided desirable intermolecular interaction leading to instant ionic gelation without addition of exogenous cross-linker and strong covalent bonds as FTIR analysis of both hydrogels showed the presence of characteristic absorptions of chitosan without any chemical reaction and confirmed the preservation of aminopolysaccharide nature and structure of chitosan. The instant gel formation is one of the key features of novel hydrogels of this study to prevent cells washout and extrusion. Furthermore, the formulated hydrogels possess pH and osmolality in accordance with cellular niche and physiological environment that resulted in high cell viability and good cell growth and proliferation of hADSCs laden in these hydrogels during 21 days of culture. In addition, such combinations of materials resulted in porous hydrogels with remarkable swelling ratio that provide oxygen and nutrients transfer for cells growth adequately and also easy exit of cellular metabolic products from the hydrogels pores. The high water content of hydrogels along with proper ionic interaction resulted in flexible and viscoelastic hydrogels with adequate mechanical robustness in harmony with myocardium and regulated disintegration and removal of them after 20 days in simulated physiological environment as a suitable time for myocardial regeneration. Although the elastic modulus, porosity, swelling ratio and degradation rate of hydrogels endorsed less mechanical strength of MH sample with respect to WH sample, it was not significant. However, MTT assay and live/dead staining demonstrated more cell retention for MH samples than that for WH samples due to more access of cells to nutrients in culture media. But higher porosity and more spaces for cell growth in MH samples provided free movements and migration of cells leading to more growth and proliferations of them. Overall conclusion is that both pH-sensitive chitosan hydrogels with instant gel formation are promising candidates to develop scaffolds for cardiac tissue regeneration. But further studies, using chemical and physical stimuli for cell growth and cell differentiation toward cardiomyocyte are required.

Acknowledgement

This research did not receive any specific grant from funding agencies in the public, commercial or not-for-profit sectors.

References

1. Reis L, Chiu LLY, Feric N, Fu L, Radisic M (2014) Cardiac regeneration and repair. (1st edition), Woodhead Publishing, Cambridge.
2. Wang H, Shi J, Wang Y, Yin Y, Wang L, et al. (2014) Promotion of cardiac differentiation of brown adipose derived stem cells by chitosan hydrogel for repair after myocardial infarction. *Biomaterials* 35: 3986-3998.
3. Chen QZ, Harding SE, Ali NN, Lyon AR, Boccaccini AR (2008) Biomaterials in cardiac tissue engineering: Ten years of research survey. *Mater Sci Eng R Reports* 59: 1-37.
4. Nelson DM, Ma Z, Fujimoto KL, Hashizume R, Wagner WR (2012) Intramyocardial biomaterial injection therapy in the treatment of heart failure: Materials, outcomes and challenges. *Acta Biomater* 7: 1-15.
5. Liu Q, Tian S, Zhao C, Chen X, Lei I, et al. (2015) Porous nanofibrous poly(l-lactic acid) scaffolds supporting cardiovascular progenitor cells for cardiac tissue engineering. *Acta Biomater* 26: 105-114.
6. Shevach M, Soffer-Tsur N, Fleischer S, Shapira A, Dvir T (2014) Fabrication of omentum-based matrix for engineering vascularized cardiac tissues. *Biofabrication* 6: 24101.
7. Navaei A, Truong D, Heffernan J, Cutts J, Brafman D, et al. (2016) PNIPAAm-based biohybrid injectable hydrogel for cardiac tissue engineering. *Acta Biomater* 32: 10-23.
8. Reis LA, Chiu LLY, Liang Y, Hyunh K, Momen A, et al. (2012) A peptide-modified chitosan-collagen hydrogel for cardiac cell culture and delivery. *Acta Biomater* 8: 1022-1036.
9. Navaei A, Saini H, Christenson W, Sullivan RT, Ros R, et al. (2016) Gold nanorod-incorporated gelatin-based conductive hydrogels for engineering cardiac tissue constructs. *Acta Biomater* 41: 133-146.
10. Annabi N, Selimović S, Acevedo Cox JP, Ribas J, Afshar Bakooshi M (2013) Hydrogel-coated microfluidic channels for cardiomyocyte culture. *Lab Chip* 13: 3569.
11. Van Vlierberghe S, Dubrue P, Schacht E (2011) Biopolymer-based hydrogels as scaffolds for tissue engineering applications: A review. *Biomacromolecules* 12: 1387-1408.
12. Reis L, Chiu, Feric N, Fu L, Radisic M (2014) *Injectable biomaterials for cardiac regeneration and repair*. (1st edition), Woodhead Publishing, Cambridge.
13. Zhang YS, Khademhosseini A (2017) *Advances in engineering hydrogels*. *Science* 356: 3627.
14. Russo V, Young S, Hamilton A, Amsden BG, Flynn LE (2014) Mesenchymal stem cell delivery strategies to promote cardiac regeneration following ischemic injury. *Biomaterials* 35: 3956-3974.
15. Li Z, Guo X, Palmer AF, Das H, Guan J (2012) High-efficiency matrix modulus-induced cardiac differentiation of human mesenchymal stem cells inside a thermosensitive hydrogel. *Acta Biomater* 8: 3586-3595.
16. Wu J, Zeng F, Huang XP, Chung JCY, Konecny F (2011) Infarct stabilization and cardiac repair with a VEGF-conjugated, injectable hydrogel. *Biomaterials* 32: 579-586.
17. Li Z, Guo X, Matsushita S, Guan J (2011) Biomaterials Differentiation of cardiosphere-derived cells into a mature cardiac lineage using biodegradable poly(N-isopropylacrylamide) hydrogels. *Biomaterials* 32: 3220-3232.
18. Tan R, She Z, Wang M, Fang Z, Liu Y, et al. (2012) Thermo-sensitive alginate-based injectable hydrogel for tissue engineering. *Carbohydr Polym* 87: 1515-1521.
19. Devolder R, Antoniadou E, Kong H (2013) Enzymatically cross-linked injectable alginate-g-pyrrole hydrogels for neovascularization. *J Control Release* 172: 30-37.
20. Landa N, Miller L, Feinberg MS, Holbova R, Shachar M (2008) Effect of injectable alginate implant on cardiac remodeling and function after recent and old infarcts in rat. *Circulation* 117: 1388-1396.
21. Pok S, Myers JD, Madhally SV, Jacot JG (2013) A multi-layered scaffold of a chitosan and gelatin hydrogel supported by a PCL core for cardiac tissue engineering. *Acta Biomater* 9: 5630-5642.
22. Habib M, Shapira-Schweitzer K, Caspi O, Gepstein A, Arbel G (2011) A combined cell therapy and *in situ* tissue-engineering approach for myocardial repair. *Biomaterials* 32: 7514-7523.
23. Tous E, Ifkovits JL, Koomalsingh KJ, Shuto T, Soeda T (2011) Influence of injectable hyaluronic acid hydrogel degradation behavior on infarction induced ventricular remodeling. *Biomacromolecules* 12: 4127-4135.
24. Henning PJ, Khan A, Jimenez E (2015) Chitosan hydrogels significantly limit left ventricular infarction and remodeling and preserve myocardial contractility. *J Surg Res*, pp: 1-8.
25. Lee S, Valmikinathan CM, Byun J, Kim S, Lee G (2015) Enhanced therapeutic neovascularization by CD31-expressing cells and embryonic stem cell-derived endothelial cells engineered with chitosan hydrogel containing VEGF-releasing microtubes. *Biomaterials* 63: 158-167.
26. Li J, Shu Y, Hao T, Wang Y, Qian Y, et al. (2013) A chitosan-glutathione based injectable hydrogel for suppression of oxidative stress damage in cardiomyocytes. *Biomaterials* 34: 9071-9081.
27. Liu Z, Wang H, Wang Y, Lin Q, Yao A, et al. (2012) The influence of chitosan hydrogel on stem cell engraftment, survival and homing in the ischemic myocardial microenvironment. *Biomaterials* 33: 3093-3106.
28. Chiu LLY, Radisic M (2011) Controlled release of thymosin β 4 using collagen-chitosan composite hydrogels promotes epicardial cell migration and angiogenesis. *J Control Release* 155: 376-385.
29. Annabi N, Tsang K, Mithieux SM, Nikkiah M, Ameri A, et al. (2013) Highly elastic micro patterned hydrogel for engineering functional cardiac tissue. *Adv Funct Mater* 23: 4950-4959.
30. Wang JJ, Christman KL (2014) *Hydrogels for cardiac repair*. Woodhead Publishing Limited, Cambridge.
31. Sepantafar M, Maheronnaghsh R, Mohammadi H, Rajabi-Zeleti S, Annabi N, et al. (2015) Stem cells and injectable hydrogels: Synergistic therapeutics in myocardial repair. *Biotechnol Adv* 34: 362-379.
32. Dai YN, Li P, Zhang JP, Wang AQ, Wei Q (2008) Swelling characteristics and drug delivery properties of nifedipine-loaded pH sensitive alginate-chitosan hydrogel beads. *J Biomed Mater Res Part B Appl Biomater* 86: 493-500.
33. Low ZW, Chee PL, Kai D, Loh XL (2015) The role of hydrogen bonding in alginate/poly(acrylamide-co-dimethylacrylamide) and alginate/poly(ethylene glycol) methyl ether methacrylate-based tough hybrid hydrogels. *RSC Adv* 5: 57678-57685.
34. Kushwaha SKS, Rai AK, Singh S (2013) Thermosensitive hydrogel for controlled drug delivery of anticancer agents. *Int J Pharm Pharm Sci* 5: 547-552.
35. Dahlmann J, Krause A, Möller L, Kensah G, Möwes M, et al. (2013) Fully defined *in situ* cross-linkable alginate and hyaluronic acid hydrogels for myocardial tissue engineering. *Biomaterials* 34: 940-951.
36. Thankam FG, Muthu J (2015) Alginate-polyester comonomer based hydrogels as physiochemically and biologically favorable entities for cardiac tissue engineering. *J Colloid Interface Sci* 457: 52-61.
37. Seo JS, Kim YJ, Cho JM, Baek E, Lee GM (2013) Effect of culture pH on recombinant antibody production by a new human cell line, F2N78, grown in suspension at 33°C and 37°C. *Appl Microbiol Biotechnol* 97: 5283-5291.
38. Kent JA. *Kent and Ruegel's Handbook of Industrial Chemistry and Biotechnology*. (11th edition), Springer, New York.
39. Parida UK, Binhani BK, Nayak PL, Nayak AK (2010) Synthesis and characterization of chitosan-polyvinyl alcohol blended with cloisite 30b for controlled release of the anticancer drug. *J Biomater Nanobiotechnol* 2: 414-425.
40. Mendes LC, Ribeiro GL, Marques RC (2012) *In situ* hydroxyapatite synthesis: influence of collagen on its structural and morphological characteristic. *Mater Sci Appl* 3: 580-586.
41. Nilsen-Nygaard J, Strand S, Vårum K, Draget K, Nordgård C (2015) Chitosan: Gels and interfacial properties. *Polymers (Basel)* 7: 552-579.
42. Yang X, Yang K, Wu S, Chen X, Yu F, Li J, et al. (2010) Cytotoxicity and wound healing properties of PVA/ws-chitosan/glycerol hydrogels made by irradiation followed by freeze-thawing. *Radiat Phys Chem* 79: 606-611.

-
43. Radhakrishnan J, Krishnan UM, Sethuraman S (2014) Hydrogel based injectable scaffolds for cardiac tissue regeneration. *Biotechnol Adv* 32: 449-461.
 44. Li Z, Guan J (2011) Hydrogels for cardiac tissue engineering. *Polymers (Basel)* 3: 740-761.
 45. Ghiaseddin A, Pouri H, Soleimani M, Vasheghani-Farahani E, Ahmadi Tafti H, et al. (2017) Cell laden hydrogel construct on-a-chip for mimicry of cardiac tissue *in vitro* study. *Biochem Biophys Res Commun* 484: 225-230.
 46. Villanueva I, Bishop NL, Bryant SJ (2009) Medium osmolarity and pericellular matrix development improves chondrocyte survival when photoencapsulated in poly(ethylene glycol) hydrogels at low densities. *Tissue Eng Part A* 15: 3037-3048.
 47. Ganji F, Vasheghani-Farahani S, Vasheghani-Farahani E (2010) Theoretical description of hydrogel swelling: A Review. *Iran Polym J* 19: 375-398.
 48. Chen SH, Tsao CT, Chang CH, Lai YT, Wu MF, et al. (2013) Synthesis and characterization of reinforced poly(ethylene glycol)/chitosan hydrogel as wound dressing materials. *Macromol Mater Eng* 298: 429-438.